Published in final edited form as:
Nat Neurosci. 2005 August ; 8(8): 1022–1027.

Ephrin-As and neural activity are required for eye-specific patterning during retinogeniculate mapping

Cory Pfeiffenberger[1], **Tyler Cutforth**[2], **Georgia Woods**[1], **Jena Yamada**[1], **Rene' C. Renteri'a**[3], **David R. Copenhagen**[3], **John G. Flanagan**[4], and **David A. Feldheim.**[1]

1*Department of Molecular, Cellular, and Developmental Biology, University of California at Santa Cruz, Santa Cruz, California 95064*

2*Center for Neurobiology and Behavior, Columbia University Medical Center, New York, New York 10032*

3*Department of Ophthalmology and Department of Physiology, University of California School of Medicine, San Francisco San Francisco, California 94143-0730*

4*Department of Cell Biology and Program in Neuroscience, Harvard Medical School, Boston, Massachusetts 02118*

Abstract

In mammals, retinal ganglion cell projections initially intermingle and then segregate into a stereotyped pattern of eye-specific layers in the dorsal lateral geniculate nucleus (dLGN). We show here that, in mice deficient for ephrin-A2, ephrin-A3, and ephrin-A5, eye-specific inputs segregate but the shape and location of eye-specific layers is profoundly disrupted. In contrast, mice that lack correlated retinal activity do not segregate eye-specific inputs. Inhibiting correlated neural activity in ephrin mutants leads to overlapping retinal projections located in inappropriate regions of the dLGN. Thus, ephrin-As and neural activity act together to control patterning of eye-specific retinogeniculate layers.

In the mammalian visual system, retinal ganglion cells (RGCs) project to their main forebrain target, the dLGN of the thalamus, in an orderly and stereotypical manner. This order is established during development and can be described by two main components. First, the projection pattern from each eye is topographic, with neighboring RGCs connecting to neighboring positions in the dLGN. The Eph family of receptor tyrosine kinases and their cell surface-bound ligands, the ephrins, have been shown to act as graded labels that are required for topographic mapping in multiple areas in the CNS, including the two main targets of RGCs: the dLGN and the superior colliculus (SC)[1–5].

The second organizing feature of visual connectivity is the segregation of projections from each eye, a phenomenon thought to depend mechanistically on neural activity. Early in development the retinogeniculate projections of the two eyes overlap but then segregate and form eye-specific layers postnatally[6,7]. Inhibiting activity in the retina or in the whole brain prevents the segregation of RGC axons[8–10]. Neural activity has been theorized to drive axon-axon competition for dLGN territory between the two eyes, and indeed, when the balance of activity levels in the two eyes is altered, inputs from the more active eye occupy a larger area within the dLGN[10–14]. It is thought that activity-based competition relies on the ability of inputs from each eye to cooperate with one another to strengthen synaptic connections in a Hebbian manner, although exactly how activity functions in this context remains controversial[15,16].

Correspondence to: David A. Feldheim..

While activity-dependent models can account for how eye-specific inputs segregate, they cannot explain the stereotypical placement of the layers within the dLGN. Segregation models based solely on neural activity predict that layer placement should be stochastic, such that in some animals a given layer of the dLGN would be innervated from the left eye while in other animals it would be innervated by the right eye, or alternatively, that axons from each eye would segregate in a "salt and pepper" pattern[17,18]. Multiple theories have been proposed to explain the stereotypical placement of the eye-specific layers, including temporal differences between ipsi- and contralateral ingrowth into the dLGN, layer-specific molecular labels, and eye-specific axon guidance molecules[18–21].

Here we test whether ephrins are important for the segregation of eye inputs within the mouse dLGN. EphA receptors and ligands are expressed in opposing gradients along the nasotemporal axis in the retina and also across the recipient SC and dLGN axes. Ephrin-A2 and ephrin-A5 are the predominant ephrin-A ligands present in the SC and dLGN and are required in vivo for topographic mapping of RGCs along these axes[1,2,5,22]. To test the relative contributions of ephrins and presynaptic activity toward the development of retinogeniculate projections, we analyzed retinal inputs to the dLGN in three populations: ephrin-A mutants, wild-type mice without correlated presynaptic activity, and ephrin-A mutants without correlated presynaptic activity.

RESULTS

Ephrin-A expression in the developing retinogeniculate projection

Multiple EphA receptors and ephrin-A ligands are expressed in gradients in the developing retinogeniculate projection (Fig.1 and Supplementary Fig. 3). In the RGC layer of the retina, EphA5 and EphA6 are expressed in a temporal>nasal gradient, whereas ephrin-A5 is expressed in the opposite nasal>temporal gradient. Ephrin-A2 and ephrin-A3 are expressed in RGCs but not in an obvious gradient (data not shown). In the dLGN, ephrin-A2 and ephrin-A5 are expressed in a ventral-lateral-anterior>dorsal-medial-posterior gradient (along the nasal-temporal mapping axis), whereas EphA7, and possibly other EphA receptors are expressed in a counter gradient. Ephrin-A3 is expressed at low levels in the dLGN[2,3](Fig. 1). In order to test the role of ephrin-A ligands in the mapping of the retinogeniculate projection, we created ephrin-A2/A3/A5 triply mutant mice by crossing ephrin-A2/A5 doubly mutant mice with ephrin-A3 mutant mice[1,23]. These mice can be viable and fertile, although a significant number of triple mutants die in utero. We first tested whether ephrin-A2, ephrin-A3, and ephrin-A5 account for the bulk of expression of ephrin-As in the dLGN by treating wild-type or triple mutant coronal thalamic sections with a soluble EphA3-alkaline phosphatase (EphA3-AP) probe that binds to all ephrin-A proteins[24]. At post-natal day 0 (P0), EphA3-AP recognizes a ventral-lateral > dorsal-medial gradient of ephrin-As throughout the dLGN (Fig. 1d), consistent with their role in topographic mapping[2]. At P6, we find that ephrin-A protein becomes restricted to contralateral input area of the dLGN(Fig. 1f–h). At all ages tested, EphA3-AP staining in the dLGN is abolished in ephrin-A2/A3/A5 triple mutants (Fig. 1e, data not shown).

Retinogeniculate projections in ephrin-A2/A3/A5 triply mutant mice

To determine if ephrin-As play a role in the placement and segregation of eye-specific layers in the dLGN, we used a two-color whole eye-fill tracing paradigm which allowed us to test the location of each eye's projections in the dLGN and quantify defects in the segregation of inputs[18]. We compared the retinal innervation patterns in the dLGN from wild-type mice and from mice lacking combinations of ephrin-A ligands, including ephrin-A2/A3/A5 triply mutant mice[1,22,23]. As shown by others, we find that the inputs from each eye are segregated in wild-type adult mice, with a single ipsilateral patch located in the dorsomedial quadrant of the dLGN[7] (Fig. 2 a,c,e). This pattern of innervation was also seen in ephrin-A2, ephrin-A3, and

ephrin-A5 single mutants, and ephrin-A3/A5 and ephrin-A2/A3 double mutants (data not shown). In contrast, ephrin-A2/A5 double mutants and ephrin-A2/A3/A5 triple mutants have severe defects in the location of the layers in the dLGN, but the segregation of inputs from each eye still occurs (Fig. 2 and Supplementary Fig. 1). Therefore, ephrin-A ligands are required for ipsilateral patch location but not the segregation of eye inputs in the dLGN.

In ephrin-A2/A3/A5 triply mutant mice, the ipsilateral patch expands along the entire dorsoventral axis of the dLGN, roughly corresponding to the nasotemporal mapping axis of the retina[25]. This phenotype is more severe in ephrin-A2/A3/A5 triple mutants than in ephrin-A2/A5 double mutants (Fig. 2c), suggesting that ephrin-A3 contributes to ipsilateral patch location through its expression either in the dLGN, on retinal axons, or both. Three-dimensional reconstruction analysis of triply mutant dLGNs shows that the ipsilateral projections are continuous and shaped like a branching tube (Supplementary videos 1 and 2). Notably, the ipsilateral projection does not appear to be random in the absence of ephrin-As. In all triple mutants examined, the ipsilateral projection branches and forms medial and central patches, although the exact location of these patches varies slightly from animal to animal. Additionally, the two dLGNs of the same mouse show symmetrical placement defects (Fig. 2b and Supplementary Fig. 1). This symmetrical positioning of the ipsilateral patch is reminiscent of the global symmetry of ocular dominance columns in the squirrel monkey[26], whereby column placement differs among individual monkeys but the column pattern is symmetric within an individual. These findings may indicate that there are additional molecules that participate in layer positioning.

It is possible that the improper ipsilateral patch location seen in ephrin-A2/A3/A5 triply mutant mice could be due to misrouting of axons at the optic chiasm. Nasal axons that normally cross would instead remain ipsilateral and map to their normal “contralateral” termination zone, leading to an “ipsi” patch located in the wrong position. If this were true we would expect a greater amount of ipsilateral axons in the dLGN. We compared the ratio of ipsilateral patch area to total dLGN area and saw no significant difference between wild-type and ephrin-A2/A3/A5 triple mutants (Fig. 2d). This suggests that the defect seen in ephrin-A2/A3/A5 mutants is not due to a larger ipsilateral projection into the dLGN or to defects in axon pruning within the dLGN. We also sectioned through the chiasm of mutant animals after labeling each eye’s inputs and saw no obvious defects in the amount of crossing. Finally, we took advantage of the SC being an exposed structure in early post-natal mice and retrogradely labeled the ipsilateral retina with an injection of DiI into the SC. In both the retinogeniculate and retinocollicular projections the majority of ipsilateral axons arise from the ventral-temporal retina[27], and this was true in ephrin-A2/A3/A5 triple mutants (Supplementary Fig. 2). Taken together these experiments suggest that ephrin-As are not required for chiasm recognition.

In wild-type mice, axons from the two eyes are intermixed at birth and then segregate by P10[6,7]. If coarse topography is a prerequisite for eye-specific segregation one might expect that the segregation of inputs would be delayed or abolished in ephrin-A2/A3/A5 triply mutant mice. Even though adult ephrin-A2/A3/A5 triply mutant mice exhibit segregated inputs (Fig. 2), we examined if ephrin-As play a role in the normal developmental timing of segregation by performing a time course experiment in which we traced retinal inputs into the dLGN from P4 through adulthood and quantified the percent of ipsilateral projection area that overlaps with contralateral projection area. In wild-type P4 mice, 92 percent of the dLGN that receives ipsilateral input also contains inputs from the contralateral eye (Fig. 3a,i). Consistent with the findings of others, this overlap decreases with post-natal age and reduces to 15 percent overlap in adults[17]. Ipsilateral triple mutant inputs are erroneously positioned as early as P4, before segregation occurs. Despite these errors, segregation of inputs occurs by P10, similar to wild-type animals (Fig. 3i), suggesting that coarse topography is not a prerequisite for the segregation of eye inputs in the LGN.

Ephrin-As and neural activity combine to pattern retinal projections

Retinal activity is thought to be important for both the establishment and maintenance of eye-specific segregation. Studies in which activity, or molecules thought to act downstream of activity, have been disrupted show that overlap of eye inputs occurs primarily in the dorsal dLGN[7,10,28,29]. To determine if altering presynaptic activity in ephrin-A mutants allows eye-specific inputs to overlap in all regions of the dLGN, we injected epibatidine into both eyes of neonatal pups and assayed the retinogeniculate projection at P9 (see Materials and Methods). Epibatidine is a nACh receptor agonist that blocks correlated RGC spiking and all calcium waves in vitro by receptor desensitization, and disrupts eye-specific segregation in both ferrets and mice[7,10,18]. Epibatidine injection into both eyes of wild-type mice every 24 hours from P3 to P7 prevents segregation at P9 (98% of ipsilateral dLGN area has overlapping contralateral projections compared to 53% in PBS injected controls). Although there is some spread of ipsilateral axons into more ventral regions of the dLGN, the overlap is predominantly in the dorsal dLGN (Fig. 4b,f). This agrees well with studies in mice and ferrets that used epibatidine to assay the role of activity in eye-specific segregation[7,10,18,25]. Epibatidine prevents eye-specific segregation to a similar degree in ephrin-A2/A3/A5 triple mutants compared to wild-type, but in triple mutants the overlap extends significantly into the ventral dLGN (Fig. 4c–f). This shows that a combination of molecular labels and neural activity act to determine the placement and segregation of eye-specific inputs within the dLGN, and indicates that in the absence of ephrin-As and correlated neural activity, regions of the dLGN that are normally occupied by the contralateral eye become competent for innervation from either eye.

Relationships between ephrin-A function and neural activity

Since it was recently shown that spontaneous bursting activity in the developing spinal cord regulates EphA4 expression on chick motor axons[30], we tested if EphA receptors in the retina change their expression after inter-retinal injection of epibatidine. We did this in two different ways. First we isolated total retinal RNA from animals injected with epibatidine or PBS (every 24 hrs from P3–P5), then performed reverse transcriptase PCR. We saw no difference in expression of EphA4, EphA5, or EphA6 under these conditions (data not shown). Second, we found no qualitative difference in the spatial distribution of Eph receptors in the retina or ephrin-A ligands in the dLGN following epibatidine injection as assayed by RNA in situ hybridization (Supplementary Fig. 3). These experiments show that epibatidine does not have a significant effect on EphA or ephrin-A expression in the retina or the dLGN; however, these techniques cannot discount Eph/ephrin post-transcriptional regulation by neural activity.

To test if neural activity patterns in the retina are affected in ephrin-A2/A3/A5 triply mutant mice, we compared the patterns of neural activity between wild-type and ephrin-A2/A3/A5 triple mutants by recording extracellularly from P4 retinas using a multielectrode array. Like wild-type, ephrin-A2/A3/A5 RGCs have bursts of action potentials followed by long periods of silence (Fig. 5a). These bursts were highly correlated among nearby RGCs as propagating waves traveled across the recorded retinal area. The addition of 10 nM epibatidine blocked the waves but did not eliminate spontaneous activity. The activity of neighboring RGCs is highly correlated and the degree of correlation for small time windows decreases over distance[31,32]. Notably, triply mutant retinas had a higher level of correlation at larger distances in the array than the wild-type retinas (Fig. 5b). This effect is likely due to the waves being somewhat broader and wider in the triple mutant, which could mean that ephrin-As are somehow required for the normal development of the inner retinal circuitry responsible for the waves. Nevertheless, segregation of eye-specific inputs in the dLGN occurred in the presence of the retinal waves in triply mutant mice.

Discussion

The patterning of RGCs within the dLGN involves correct topographic location of contra and ipsilateral axons, segregation of right and left eye inputs, and the establishment and placement of eye-specific layers. The relative contributions of activity-dependent and independent mechanisms to each of these aspects of mapping have long been debated. We and others have shown that EphA receptors and ephrin-A ligands are required for topographic mapping of the nasal-temporal axis of the retina onto both the SC and the dLGN[1–3,22]. This study shows that ephrin-As are also required for the proper placement of eye-specific inputs in the mouse dLGN, but are not essential for the segregation of these inputs. In agreement with others, we find that correlated retinal activity is required for the segregation of eye-specific inputs. Notably, we find that the ephrin-A mediated aspects of mapping (topography and layer placement) act independently of the activity-dependent segregation of inputs. Ephrin-A2/A3/A5 triply mutant mice have severe defects in layer placement but still segregate eye inputs in the dLGN with normal developmental timing. In addition, we show that inhibiting correlated presynaptic retinal activity in ephrin-A2/A3/A5 triply mutant mice abolishes both segregation and layer placement, indicating that the combination of ephrin-As and presynaptic neural activity is necessary to pattern one axis of the retinogeniculate projection. Our analysis of ephrin mutant mice leads us to a model whereby a combination of topographic mapping molecules and neural activity-dependent events are parallel mechanisms that together create the stereotypical connectivity patterns in the primary visual system (Supplementary Fig. 4).

How might ephrin-As guide the ipsilateral axons to the appropriate place? One possibility is that ipsilateral axons are directed to a specific region of the dLGN by a unique combination of A–P and D–V topographic labels. Ipsilateral axons arise from the ventrotemporal retina, which has high EphA and EphB receptor expression. Therefore, gradients of ephrin-A2 and ephrin-A5 along one axis of the dLGN, combined with an orthogonal gradient of ephrin-Bs, could steer ipsilateral axons their final location in the dLGN. Alternatively, ephrin-As could act as topographic labels during the topographic mapping phase of dLGN development, and then act as layer placement labels during the segregation phase. Notably, at P6, ephrin-As are predominantly expressed in the ventrolateral dLGN where they may act to repel ipsilateral axons toward their location in the dorsomedial dLGN (Fig. 1f–h). This expression may be due to changes in ephrin-A expression in dLGN neurons, or to ephrin-A ligands present on newly arriving nasal RGC axons. Layer-specific expression of ephrin-A ligands has also been observed in the ferret, where topographic mapping is established at birth and eye-specific segregation occurs postnatally between P1 and P10. During the period of eye-specific segregation in ferrets, ephrin-A5 expression is higher in the ipsilateral layer than in the contralateral layer of the dLGN, and ectopic expression of EphA receptors in the postnatal retina causes layering errors (Huberman et al., accompanying manuscript). Therefore, just as ephrin gradients have evolved for use in multiple visual targets[2] and are proposed to act first in the intermediate target and later in the final target in thalamic-cortical mapping[4], they may be used in multiple aspects of mapping within a particular visual target.

The relative contributions of guidance cues and neural activity to the functional wiring of the nervous system have long been debated. Here we show, in the model projection from the retina to the dLGN, that both are required for normal wiring. It will be interesting to see if the development of structures in the cerebral cortex, such as the formation of cortical columns, will also employ a combination of ephrins and neural activity during development.

Materials and Methods

Animals were maintained in the animal facility at UC Santa Cruz and used in accordance with protocols approved by the UC Santa Cruz Institutional Animal Care and Use Committee.

Whole eye labeling and visualization of the dLGN—2–3 μl of a 2mg/ml solution of cholera toxin B-Alexa Fluor 594 or cholera toxin B-Alexa Fluor 488 (Molecular Probes) in PBS was injected into the eye using a pulled pipette adapted to a Picospritzer III pressure injection system (Parker Hannifin Corporation). Mice were sacrificed two or three days later, intercardially perfused with 4% paraformaldehyde in PBS and the brains were fixed overnight. Brains were embedded in 2–3% agarose (Sigma) in PBS and 150–200 μm coronal sections were cut using a vibratome (World Precision Instruments Inc.). Images were captured with an AxioCam Hrm digital camera through a 20x objective on an Axioskop 2 Plus microscope (Zeiss) and merged using Adobe Photoshop. For 3–D confocal reconstruction analysis,100μm coronal sections were cut on a vibratome and mounted on glass slides with Fluoromount-G (Southern Biotech.) overnight in the dark. 10μm optical sections from 5 serial sections per brain were imaged on an Axiovert 200 inverted microscope (Zeiss) through the "LSM 5 Pascal" laser scanning module. Images were acquired into the accompanying LSM 5 Pascal software, then stacked anterior to posterior using Image J (http://rsb.info.nih.gov/ij/).

Quantification of overlap of projections—Image J was first used to reduce background with a rolling ball filter of 250 pixels. The dLGN was then selected and isolated so that further manipulations were only on this region, disregarding the optic tract and vLGN. The isolated dLGNs were then thresholded in an unbiased manner that discarded the pixels in the lowest intensity quintile, as determined by histogram analysis. This approach sufficiently eliminates background while creating a binary image that closely mimics the predicted structure of the unthresholded projections. The thresholded ipsilateral and contralateral images were then compared using the image calculator "OR" function and the area of the resulting image was determined to be "overlap". Percent dLGN containing overlap = (overlap/total dLGN area) x 100; percent ipsilateral projections containing overlapping contralateral projections = (overlap/total ipsilateral area) x 100. To quantitate the length of the dLGN, a line was drawn at an angle from the dorsal–medial dLGN to the vLGN to yield the maximum dimension of the dLGN in each section. Ipsilateral projection placement along that line was then measured. Percent dLGN length = (total length of the ipsilateral projection) /(total length of the dLGN) x 100. All quantification of dLGN projections was done blind to treatment and genotype.

Epibatidine injections—To image overlap at P9:1–2 μl of 1mM epibatidine in PBS (Biomol) was injected intravitreally into both eyes every 24 h from P3 to P7 using a Picospritzer III. Injections at P3 and P4 were performed through the skin covering the eye; at P5 the skin was cut open to allow the three final injections to be performed through the same hole in the eye. Mice were sacrificed at P9 and processed for visualization in the same way as the whole eye fills. To collect RNA and assay EphA and ephrin-A RNA expression at P6, 1–2 μl of PBS or 1mM epibatidine in PBS was injected intravitreally into both eyes every 24 hrs from P3 to P5. The first injection was performed through the skin covering the eye, at P4 the skin was cut open to allow the final two injections to be performed through the same hole in the eye. Mice were sacrificed on P6.

In situ RNA hybridization—In situ probes for Ephrin-A5 (containing nucleotides 102–682 of the open reading frame), ephrin-A3 (containing nucleotides 100–687), and EphA7 (containing nucleotides 721–1193) were used to make antisense and sense digoxigenin labeled RNA probes. Frozen section in situ hybridization was done as previously described[2]. Stained sections were photographed using a cool-pix digital camera (Nikon) mounted onto a dissecting microscope.

Affinity Probe in Situ—EphA3-AP in situ was done as described[34]. Briefly, brains were dissected from neonatal pups and rapidly embedded in 5% agarose in PBS. 250μm coronal sections were cut using a vibratome, and those containing dLGN were treated with EphA3-AP

as floating sections. Stained sections were photographed using a cool-pix digital camera (Nikon) mounted onto a dissecting microscope.

Multielectrode extracellular recording from retina—Animals were sacrificed by at P3 to P5, after which an eye was removed. The neural retina was dissected and placed ganglion cell-side down in a recording chamber using nitrocellulose paper as support. The multielectrode chambers (MEA-60 system; Multi Channel Systems (MCS), Germany) consisted of an array of 60 planar electrodes in 8 rows spaced 100 μm apart for a total array size of 700 μm^2. Retinas were perfused at room temperature and incubated at 34°C for an hour before recordings were started, and the temperature was maintained at 34°C throughout the recordings. The saline consisted of (in mM) NaCl (124), KCl (2.5), $CaCl_2$ (2), $MgCl_2$ (2), NaH_2PO_4 (1.25), $NaHCO_3$ (26), and glucose (22.2), and the pH was maintained at 7.3 to 7.4 by bubbling with $95\%O_2/5\%CO_2$ mixed gas. Data were acquired in a response range of 0.1 Hz to 3kHz at 5 kHz (MC_Rack, v.2.0; MCS).

After recording, action potential waveforms from high-pass filtered data were clustered based on the first two principal components as described previously using a k-means algorithm (Offline Sorter, v.1.3; Plexon, Inc; Dallas, TX). The algorithm eliminated outlier waveforms at a threshold of 1.3 times the mean distance from the calculated cluster center. Obvious automatic sorting errors were corrected for each cluster manually. Timestamps for each action potential of each sorted unit were used to generate peristimulus spike rasters and to perform auto- and cross-correlation analyses (Neuro Explorer, v.2.6; Nex Technologies; Dallas, TX). Correlation indices were calculated as described[35] using custom macros (IGOR Pro, v.4.0; Wave Metrics; Lake Oswego, OR).

Supplementary Material

Refer to Web version on PubMed Central for supplementary material.

Acknowledgements

We thank B. Chapman and A. Huberman for stimulating discussions and sharing data prior to publication. We thank C. Chen, P. Vanderhaeghen and C. Mason for helpful discussions and critical reading of the manuscript, and R. Axel for support (T.C.). This work was supported by a National Institutes of Health grant EY014689 (D.A.F.), a National Institutes of Health training predoctoral training grant GM08646 (C.P.), and National Institutes of Health grants R01 DC04209 and P01 CA23767 (T.C.).

References

1. Feldheim DA, et al. Genetic analysis of ephrin-A2 and ephrin-A5 shows their requirement in multiple aspects of retinocollicular mapping. Neuron 2000;25:563–574. [PubMed: 10774725]
2. Feldheim DA, et al. Topographic guidance labels in a sensory projection to the forebrain. Neuron 1998;21:1303–1313. [PubMed: 9883724]
3. Feldheim DA, et al. Loss-of-function analysis of EphA receptors in retinotectal mapping. J Neurosci 2004;24:2542–50. [PubMed: 15014130]
4. Vanderhaeghen P, Polleux F. Developmental mechanisms patterning thalamocortical projections: intrinsic, extrinsic and in between. Trends Neurosci 2004;27:384–91. [PubMed: 15219737]
5. McLaughlin T, Hindges R, O'Leary DD. Regulation of axial patterning of the retina and its topographic mapping in the brain. Curr Opin Neurobiol 2003;13:57–69. [PubMed: 12593983]
6. Metin C, Godement P, Saillour P, Imbert M. [Physiological and anatomical study of the retinogeniculate projections in the mouse]. C R Seances Acad Sci III 1983;296:157–62. [PubMed: 6404518]
7. Rossi FM, et al. Requirement of the nicotinic acetylcholine receptor beta 2 subunit for the anatomical and functional development of the visual system. Proc Natl Acad Sci U S A 2001;98:6453–8. [PubMed: 11344259]

8. Sretavan DW, Shatz CJ, Stryker MP. Modification of retinal ganglion cell axon morphology by prenatal infusion of tetrodotoxin. Nature 1988;336:468–471. [PubMed: 2461517]
9. Shatz CJ, Stryker MP. Prenatal tetrodotoxin infusion blocks segregation of retinogeniculate afferents. Science 1988;242:87–9. [PubMed: 3175636]
10. Penn AA, Riquelme PA, Feller MB, Shatz CJ. Competition in retinogeniculate patterning driven by spontaneous activity. Science 1998;279:2108–2112. [PubMed: 9516112]
11. Sretavan DW, Shatz CJ. Prenatal development of retinal ganglion cell axons: segregation into eye-specific layers within the cat's lateral geniculate nucleus. J Neurosci 1986;6:234–51. [PubMed: 3944621]
12. Rakic P. Development of visual centers in the primate brain depends on binocular competition before birth. Science 1981;214:928–31. [PubMed: 7302569]
13. Godement P, Salaun J, Metin C. Fate of uncrossed retinal projections following early or late prenatal monocular enucleation in the mouse. J Comp Neurol 1987;255:97–109. [PubMed: 3819012]
14. Stellwagen D, Shatz CJ. An instructive role for retinal waves in the development of retinogeniculate connectivity. Neuron 2002;33:357–67. [PubMed: 11832224]
15. Crowley JC, Katz LC. Ocular dominance development revisited. Curr Opin Neurobiol 2002;12:104–9. [PubMed: 11861172]
16. Huberman AD, et al. Eye-specific retinogeniculate segregation independent of normal neuronal activity. Science 2003;300:994–8. [PubMed: 12738869]
17. Muir-Robinson G, Hwang BJ, Feller MB. Retinogeniculate axons undergo eye-specific segregation in the absence of eye-specific layers. J Neurosci 2002;22:5259–64. [PubMed: 12097474]
18. Huberman AD, Stellwagen D, Chapman B. Decoupling eye-specific segregation from lamination in the lateral geniculate nucleus. J Neurosci 2002;22:9419–29. [PubMed: 12417667]
19. Shatz. Emergence of order in visual system development. Proc Natl Acad Sci USA 1996;93:602–608. [PubMed: 8570602]
20. Crowley JC, Katz LC. Development of ocular dominance columns in the absence of retinal input. Nat Neurosci 1999;2:1125–1130. [PubMed: 10570491]
21. Chapman B. Necessity for afferent activity to maintain eye-specific segregation in ferret lateral geniculate nucleus. Science 2000;287:2479–82. [PubMed: 10741966]
22. Frisén J, et al. Ephrin-A5 (AL-1/RAGS) is essential for proper retinal axon guidance and topographic mapping in the mammalian visual system. Neuron 1998;20:235–243. [PubMed: 9491985]
23. Cutforth T, et al. Axonal ephrin-As and odorant receptors: coordinate determination of the olfactory sensory map. Cell 2003;114:311–22. [PubMed: 12914696]
24. Flanagan JG, Vanderhaeghen P. The ephrins and Eph receptors in neural development. Annu Rev Neurosci 1998;21:309–345. [PubMed: 9530499]
25. Grubb MS, Rossi FM, Changeux JP, Thompson ID. Abnormal functional organization in the dorsal lateral geniculate nucleus of mice lacking the beta 2 subunit of the nicotinic acetylcholine receptor. Neuron 2003;40:1161–72. [PubMed: 14687550]
26. Adams DL, Horton JC. Capricious expression of cortical columns in the primate brain. Nat Neurosci 2003;6:113–4. [PubMed: 12536211]
27. Williams SE, et al. Ephrin-B2 and EphB1 mediate retinal axon divergence at the optic chiasm. Neuron 2003;39:919–35. [PubMed: 12971893]
28. Pham TA, Rubenstein JL, Silva AJ, Storm DR, Stryker MP. The CRE/CREB pathway is transiently expressed in thalamic circuit development and contributes to refinement of retinogeniculate axons. Neuron 2001;31:409–20. [PubMed: 11516398]
29. Huh GS, et al. Functional requirement for class I MHC in CNS development and plasticity. Science 2000;290:2155–9. [PubMed: 11118151]
30. Hanson MG, Landmesser LT. Normal patterns of spontaneous activity are required for correct motor axon guidance and the expression of specific guidance molecules. Neuron 2004;43:687–701. [PubMed: 15339650]
31. Tian N, Copenhagen DR. Visual stimulation is required for refinement of ON and OFF pathways in postnatal retina. Neuron 2003;39:85–96. [PubMed: 12848934]

32. Demas J, Eglen SJ, Wong RO. Developmental loss of synchronous spontaneous activity in the mouse retina is independent of visual experience. J Neurosci 2003;23:2851–60. [PubMed: 12684472]

33. Hindges R, McLaughlin T, Genoud N, Henkemeyer M, O'Leary DD. EphB forward signaling controls directional branch extension and arborization required for dorsal-ventral retinotopic mapping. Neuron 2002;35:475–87. [PubMed: 12165470]

34. Flanagan JG. In situ analysis of embryos with receptor or ligand fusion protein probes. Curr Biol 2000;10:R52–R53. [PubMed: 10662675]

35. Wong ROL, Meister M, Shatz CJ. Transient period of correlated bursting activity during development of the mammalian retina. Neuron 1993;11:923–938. [PubMed: 8240814]

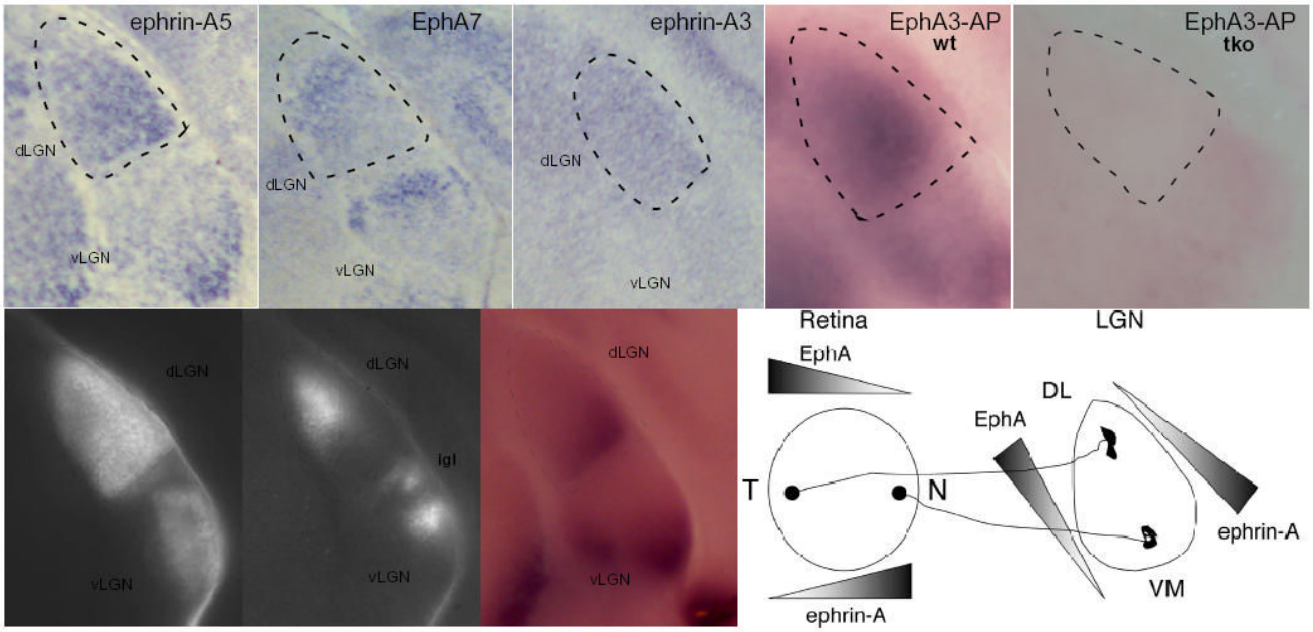

Fig 1.

Expression of EphA receptors and ephrin-A ligands in the developing mouse visual system. (a–c) Coronal sections of mouse P0 brain were treated with RNA hybridization probes for ephrin-A5 (a), EphA7 (b), and ephrin-A3 (c). (d,e) Total ephrin-A ligand expression in the developing thalamus consists of ephrin-A2, ephrin-A3, and ephrin-A5. Coronal sections were stained with EphA3-AP (to detect ephrin-A ligands) in wild-type (d), or ephrin-A2/A3/A5 triple mutants (e) at P0. Ephrin-As are expressed in gradients across the whole dLGN at these early time points. (f,g) Grey scale photomicrographs of coronal sections at P6 after injection of cholera toxin B-Alexa Fluor 594 or cholera toxin B-Alexa Fluor 488 into left and right eyes respectively showing the retinal axons from contralateral (f) and ipsilateral (g) eyes projecting into the dLGN. (h) The same section treated with EphA3-AP to detect ephrin-A ligands in the LGN at P6 showing ephrin-A expression becomes localized to ventral-lateral regions of the dLGN, which will become innervated only by contralateral inputs. No staining was ever seen when alternate sections were stained with AP alone. (i) Schematic of EphA receptor and ephrin-A ligand in the retina and dLGN during early periods of visual mapping. dLGN, dorsal lateral geniculate nucleus; vLGN, ventral lateral geniculate nucleus; igl, inter geniculate layer. N, nasal; T, temporal; VM, ventral-medial; DL, dorsal-lateral; wt, wild-type; tko, ephrin-A2/A3/A5 triple knockout. Dotted lines denote the approximate boundary of the dLGN. Dorsal is to the top, medial is to the left.

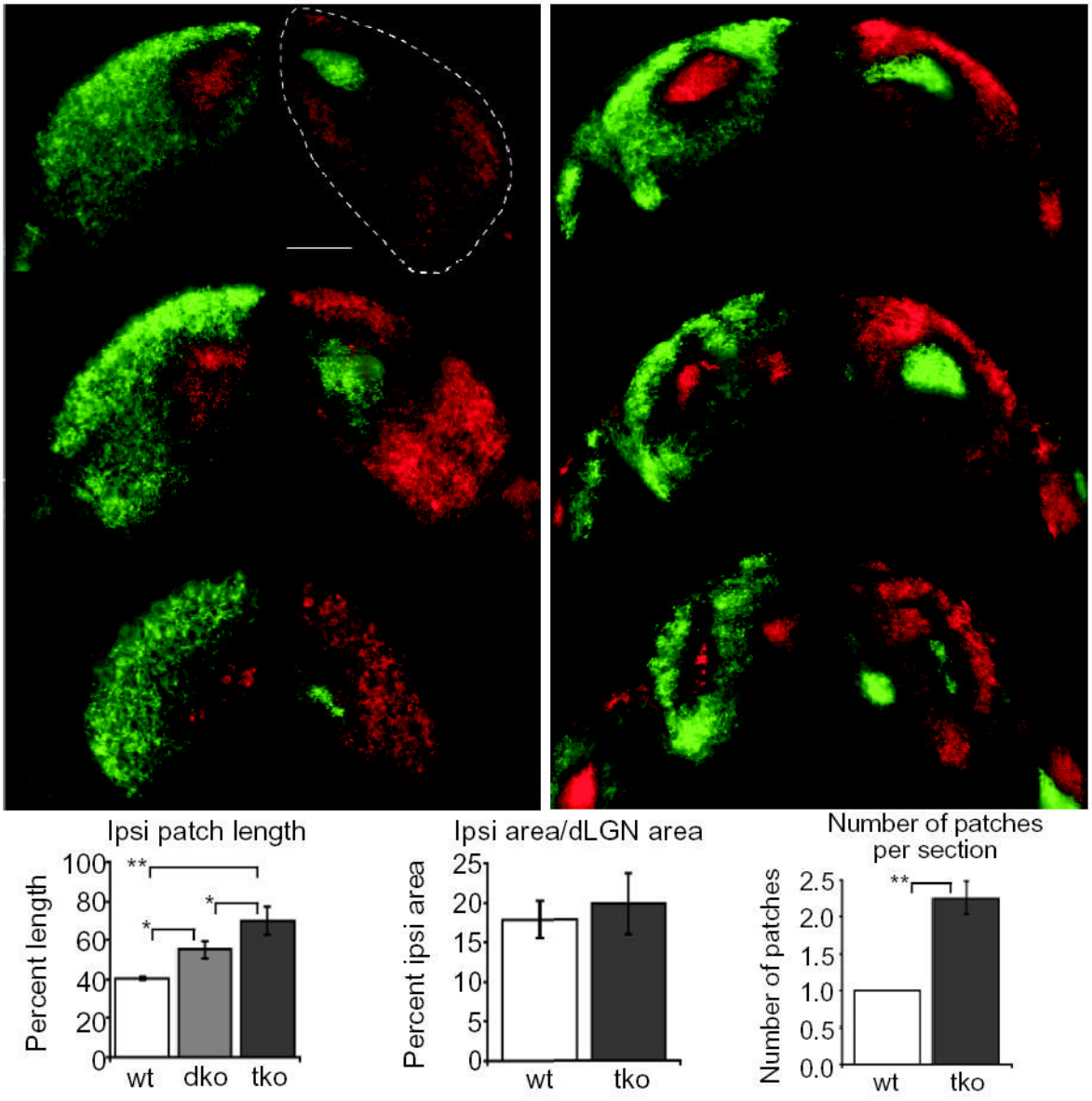

Fig 2.

Defects in eye-specific layer placement but not in eye-specific segregation in ephrin-A2/A3/A5 triply mutant mice. Axons from the right eye are shown in green, axons from the left eye are shown in red. (a,b) A series of coronal sections from anterior (top) to posterior (bottom) showing left and right dLGN in representative adult (a) wild-type (wt) and (b) ephrin-A2/A3/A5 triple knockout (tko) mice. (c) Distribution of ipsilateral axon location within the dLGN. Data are expressed as a percentage of dLGN length along the longest DM-VL axis in coronal sections from wild-type, ephrin-A2/A5 doubly mutant (dko) and ephrin-A2/A3/A5 tko mice, showing that the location of eye-specific inputs is defective in ephrin mutants. (d) Quantification of the ratio of percent ipsilateral projection area to total dLGN area in wild-type and ephrin-A2/A3/A5 tko mice showing no significant difference in ipsilateral projection amounts between these two populations of mice. (e) Quantification of the average number of ipsilateral patches seen in a coronal section. A comparison of wild-type and ephrin-A2/A3/A5 tko mice shows that the ipsilateral projection in the dLGN is patchy in ephrin tko mice. Dotted

lines show the outline of the dLGN. (* $P < 0.001$,** $P << 0.001$, ANOVA test.) (n= mice analyzed; wild-type n=3 (4 sections each from 3 mice), ephrin-A2/A5 mutant n=8 (4 sections each from 8 mice), ephrin-A2/A3/A5 mutant n=9 (4 sections each from 9 mice). Scale bar = 200μm. Dorsal is to the top.

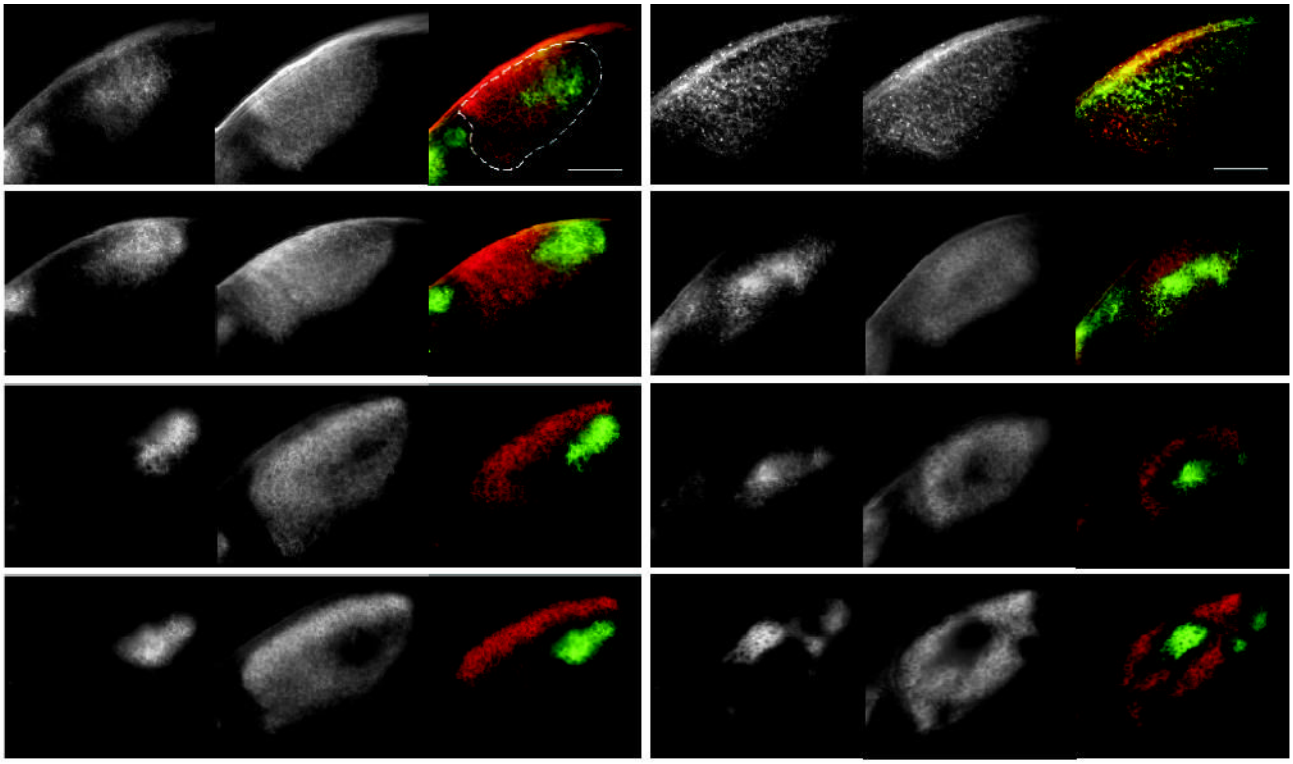

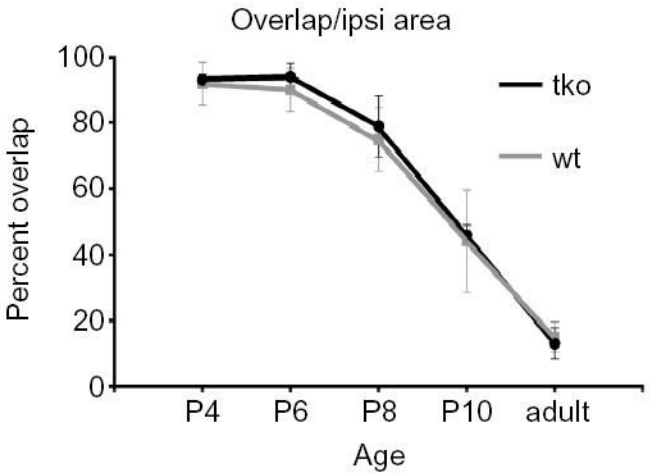

Fig 3.

Time course of eye-specific segregation in wild-type and ephrin-A2/A3/A5 tko mice. (a–h) Photomicrographs of 200μm-thick coronal sections showing the retinal projections from each eye projecting into the dLGN in wild-type (a,c,e,g) and ephrin-A2/A3/A5 tko (b,d,f,h) mice at P4 (a,b), P6 (c,d), P8 (e,f) and P10 (g,h). Each set of three images represents, from left to right: the ipsilateral projection, the contralateral projection and the merged image of one dLGN. Dorsal is to the top, medial is to the right in each image. The scale bar represents 200μm. Dotted line shows the outline of the dLGN. (i) Graphical representation of the percent of the ipsilateral area in which contralateral projections are also present (“overlap”), comparing wild-type and ephrin-A2/A3/A5 mutant mice at P4, P6, P8, P10, and adult. Error bars represent one standard

deviation in either direction. (wild-type P4, P6, P10: *n*=4 mice (16 dLGN sections); wild-type P8, adult, tko P4, P6, P8, P10, adult: *n*=3 mice (12 dLGN sections).

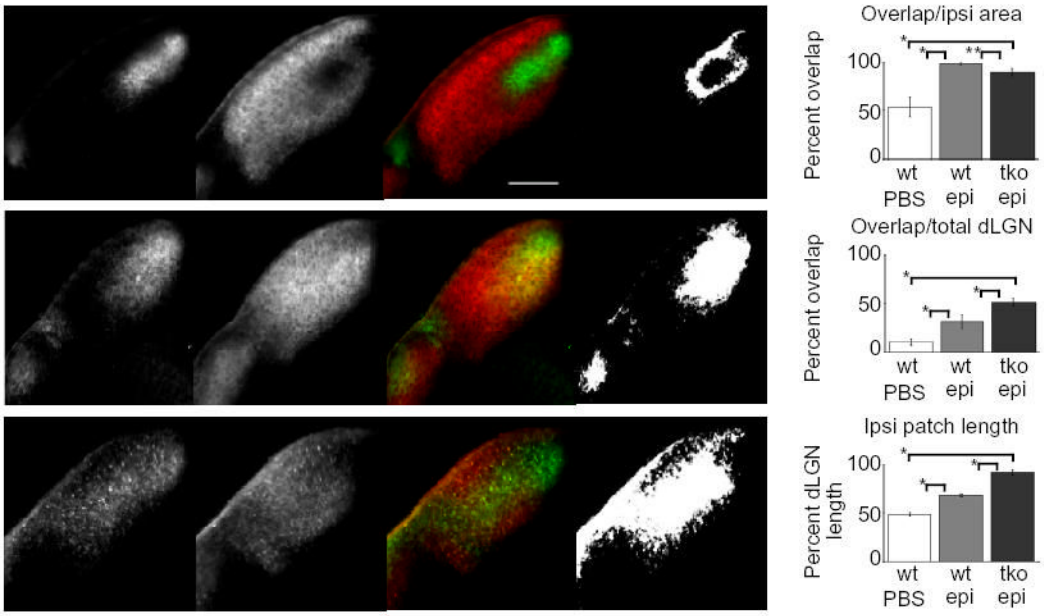

Fig 4.

Area of dLGN overlap is increased in epibatidine-treated ephrin-A2/A3/A5 mutant mice as compared to epibatidine-treated wild-type mice. (a–c) Photomicrographs of 150μm thick coronal dLGN sections from P9 wild-type (a, b) and ephrin-A2/A3/A5 mutant mice (c) that received binocular intravitreal epibatidine injections (b, c) or PBS control injections (a) every 24 hours from P3 to P7. The pictures are shown in groups of four representing, from left to right: the ipsilateral projection, the contralateral projection, the merged image and a binary image representing dLGN area with overlapping ipsilateral and contralateral projections. Dorsal is to the top, medial is to the right. The scale bar is 200μm. (d) Quantitative comparison of ipsilateral and contralateral axonal overlap between control (wt PBS), wild-type (wt epi), and ephrin-$A2^{-/-}A3^{-/-}A5^{-/-}$ or ephrin-$A2^{-/-}A3^{+/-}A5^{-/-}$ (tko epi) mutant mice, presented as the percentage of the ipsilateral area containing overlapping contralateral projections. (e) Quantitative comparison of ipsilateral and contralateral axonal overlap between control, wild-type and ephrin-$A2^{-/-}A3^{-/-}A5^{-/-}$ plus ephrin-$A2^{-/-}A3^{+/-}A5^{-/-}$ mutant mice, presented as the percentage of the total dLGN area containing overlap. (f) Quantitative comparison of the ipsilateral patch length between control, wild-type, and ephrin-$A2^{-/-}A3^{-/-}A5^{-/-}$ (or ephrin-$A2^{-/-}A3^{+/-}A5^{-/-}$) mutant mice, expressed as the percentage of the dLGN length covered by the ipsilateral patch along the DM-VL axis. (* $P << 0.001$; ** $P < 0.005$, ANOVA test) (wt +PBS, wt+Epi: n=4 mice (16 dLGN sections); ephrin-$A2^{-/-}A3^{-/-}A5^{-/-}$ plus ephrin-$A2^{-/-}A3^{+/-}A5^{-/-}$+Epi: n=4 mice (2 of each genotype, 16 dLGN sections).

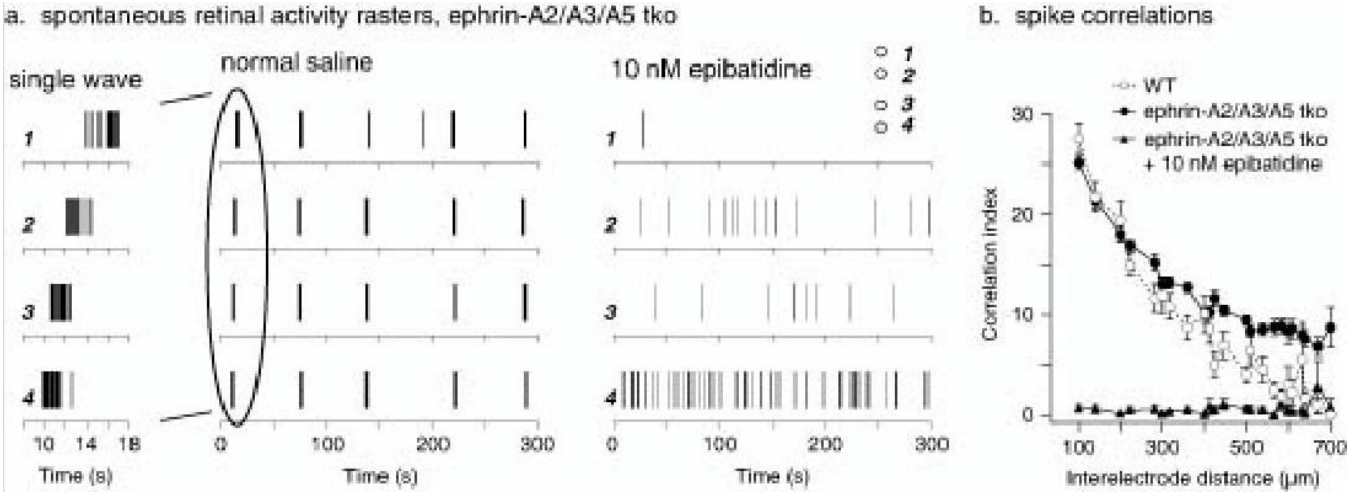

Fig 5.

Spontaneous retinal waves in ephrin-A2/A3/A5 mutant retinas. (a) Spike rasters of spontaneous retinal activity from an ephrin A2/A3/A5 triple knockout (tko) mouse at P4. Activity at single ganglion cells occurs in bursts followed by long periods of silence. Recording on a multielectrode array shows that these bursts occur across the retina in waves. Relative electrode positions (1 – 4) for the example neuron recordings are illustrated in the inset of the right panel. Closer examination of a typical wave (left panel, 10 sec) shows it traveling from electrode 4 to 1 at 140 μm/sec. In contrast, the activity of the same neurons in the presence of 10 nM epibatidine shows no waves. (b) Correlation indices were calculated for all pairs of neurons recorded from a P4 wild-type retina (white circles), a P4 ephrinA2/A3/A5 tko retina (black circles), and an epibatidine treated ephrin-A2/A3/A5 tko retina (black triangles). These are plotted against the distance between the electrodes from which the neuron's spikes were recorded. In both the wild-type and ephrin A2/A3/A5 tko retinas, wave activity led to high correlation indices at small distances and lower ones at larger distances. Ephrin A2/A3/A5 tko retinas had a higher level of correlation at the largest distances in the array (approximately 800 μm) than the wild-type retinas, due to waves that were somewhat broader. Epibatidine, which eliminated the wave activity but did not eliminate spike activity in the ephrin A2/A3/A5 tko retina, abolished correlated activity at all distances. Wild-type n=3 retinas, ephrin-A2/A3/A5 n=3 retinas.